

## Real-time measurements of trace gases using a compact difference-frequency-based sensor operating at 3.5 $\mu\text{m}$

D.G. Lancaster, D. Richter, R.F. Curl, F.K. Tittel

Rice Quantum Institute, Rice University, 6100 Main St., Houston, TX, 77005, USA  
(Fax: +1-713/524-5237, E-mail: fkt@rice.edu)

Received: 1 April 1998

**Abstract.** The use of a compact gas sensor based on cw difference-frequency generation in periodically poled LiNbO<sub>3</sub> for on-line absorption measurements of H<sub>2</sub>CO, CH<sub>4</sub>, and H<sub>2</sub>O near 3.5  $\mu\text{m}$  is reported. Formaldehyde levels of 30 ppb, corresponding to absorptions of  $2 \times 10^{-4}$  have been measured using absorption spectroscopy. In this paper we report specifically the performance of this sensor as part of the 1997 Lunar–Mars Life Support Test program at the NASA Johnson Space Center.

**PACS:** 07.88.+y; 42.62.Fi; 42.65.-k

The monitoring and detection of trace gases at the level of parts per billion in diverse fields ranging from pollution and greenhouse-gas emission, to applications involving environmental control for the workplace and space habitats has become increasingly important. One such application in which we were involved, was the 90-day Lunar–Mars comprehensive life support test conducted at the NASA Johnson Space Center, Houston. The test was undertaken in a three-level 8-m diameter, human-rated space station simulation chamber, accommodating four mission specialists. One goal of this program was to test new life-support initiatives such as advanced air and water recycling technologies that are to be used for the international space station program. The purpose of our involvement in the test was to ascertain H<sub>2</sub>CO concentration levels inside the NASA test chamber with a portable and real-time gas sensor.

The motivation for monitoring H<sub>2</sub>CO levels in a sealed, human-rated environment, is that its presence can cause headaches as well as throat and ear irritation at low concentrations (> 100 ppb). There are concerns about more serious adverse health effects at higher H<sub>2</sub>CO concentration levels. Consequently, NASA has set a stringent spacecraft maximum allowable concentration of 40 ppb for crew exposure from 7 to 180 days [1]. To reduce H<sub>2</sub>CO levels below this concentration, any outgassing materials and equipment must be identified. Hence, the development of an in situ, real-time, portable gas sensor capable of identifying H<sub>2</sub>CO emission

sources and monitoring concentrations at sub-ppm levels in air was initiated.

Further motivation for measuring H<sub>2</sub>CO concentrations precisely is that it is an important intermediate compound in tropospheric chemistry cycles, and serves as a significant source of CO in the natural troposphere with typical atmospheric levels of 300 ppt [2]. While this concentration level is about two orders of magnitude below the sensitivity limits for the monitoring apparatus described here, H<sub>2</sub>CO is also a significant byproduct of combustion devices and the present monitor is quite satisfactory for monitoring formaldehyde emissions from combustion. Accurate measurements of combustion emissions are thus important in the reduction of urban air pollution levels of formaldehyde.

For real-time measurements of trace gases, optical techniques are the most suitable and include FTIRs [3], tunable infrared laser absorption spectroscopy using either overtone absorption spectroscopy in the near-IR [4, 5], or direct infrared absorption spectroscopy in the mid-IR [6, 7] and photoacoustic spectroscopy [3]. In the mid-IR, difference-frequency generation (DFG)-based sensors have been shown to be particularly suitable for absorption spectroscopy [8, 9]. The criteria that must be considered for a system to be effective as a trace-gas sensor include adequate sensitivity for the concentrations present, the ability to discriminate from any other gases present, and reliable field operation.

Considering the monitoring of H<sub>2</sub>CO specifically, Fried et al. [10] reported a tunable diode laser absorption technique based on cryogenically cooled lead-salt diode lasers which achieved a H<sub>2</sub>CO detection sensitivity of 0.04 ppb. This is clearly a much higher sensitivity than is reported here, but it comes at the cost of cryogenic operation. Fourier transform infrared spectroscopy (FTIR) is a widespread laboratory and industrial monitoring technique, which might be made suitable for monitoring H<sub>2</sub>CO, but field FTIR spectrometers generally suffer from inadequate spectral resolution for this purpose. NASA monitors H<sub>2</sub>CO by using a chemical absorption badge capable of determining average concentrations over an extended period of time with a sensitivity  $\approx$  20 ppb. The badge is typically exposed for 24 h, and then processed using a wet chemical technique. The result obtained depends

on the exposure, which in turn depends upon the location of the badge. This can be an advantage in that it is a personal monitor, but a disadvantage in obtaining an overall assay of the air quality. A major disadvantage of badges is that there is a time required for exposure and a time required for development, which is usually an additional 24 h, and hence exposure levels are learned only after significant additional exposure. It should be noted that  $\text{H}_2\text{CO}$  is not a very suitable candidate for gas chromatographic and mass spectrometric measurement on account of its strong propensity to adsorb on surfaces.

Infrared absorption spectroscopy using a DFG source is an attractive alternative approach for the monitoring of formaldehyde, because of the inherent narrow bandwidth of the DFG source and the ability to design a monitor which is compact and operates at room temperature. In recent work, we demonstrated the feasibility of using a DFG-based sensor for sensitive  $\text{H}_2\text{CO}$  detection (to 30 ppb) [11]. In the current work several enhancements were introduced to the sensor, including on-line frequency calibration and automatic data acquisition and processing which permits unattended operation over extended periods of time.

The  $\nu_5$  fundamental band from 3.2–3.6  $\mu\text{m}$  is convenient for  $\text{H}_2\text{CO}$  detection in the mid-infrared. The specific line selected for monitoring must take into account the presence of competing absorption lines of common atmospheric constituents. For the life support test, this line selection was critical because of expected high  $\text{CH}_4$  concentration levels of up to 150 ppm inside the chamber. A suitable line was chosen at  $2831.642\text{ cm}^{-1}$  (3.5  $\mu\text{m}$ ), which also has a (5 times weaker) satellite line at  $2831.699\text{ cm}^{-1}$  using the HITRAN 96 database [12]. This line was first identified in [10] to be suitable for atmospheric sensing. The line strength of the  $\text{H}_2\text{CO}$  line is  $5.04 \times 10^{-20}\text{ cm/molecule}$  [HITRAN 96] at  $2831.642\text{ cm}^{-1}$ . The predicted absorption is  $2 \times 10^{-4}$ , assuming a concentration of 30 ppb and absorption path of 18 m. Because of the proximity of a methane line close by ( $0.080\text{ cm}^{-1}$ ) at  $2831.562\text{ cm}^{-1}$  and a water line at  $2831.841\text{ cm}^{-1}$ , the absorption measurements are carried out at reduced pressure (typically 95 Torr) to reduce pressure broadening and to resolve the individual spectral lines. A HITRAN 96 simulation of this spectral region is shown in Fig. 1. A minor advantage of the choice of this spectral region is the presence of a well-isolated  $\text{CH}_4$  line at  $2829.592\text{ cm}^{-1}$ , which allowed this species to be monitored in the chamber. The line at  $2830.008\text{ cm}^{-1}$  can be used to monitor  $\text{H}_2\text{O}$ . These infrared spectral absorptions could be conveniently accessed by varying the laser diode temperature by  $< 1.3\text{ }^\circ\text{C}$ .

For the sensor described here, the detection sensitivity using direct absorption spectroscopy is limited by the baseline irregularities caused by the occurrence of accidental etalons that occur in the beam path and not by detector noise or insufficient mid-IR power levels. This fact made it pointless to use the alternative spectroscopic techniques of frequency or wavelength modulation spectroscopy [13, 14] in which the frequency of the IR source is modulated and the signal detected at one of the harmonics of the modulation frequency. Although this technique reduces the  $1/f$  noise inherent in the detection circuit, the frequency modulation technique is also limited by the presence of etalons in the beam path. Therefore we expected no significant improvement in sensitivity by the use of frequency modulation over the simpler direct absorption technique and did not explore

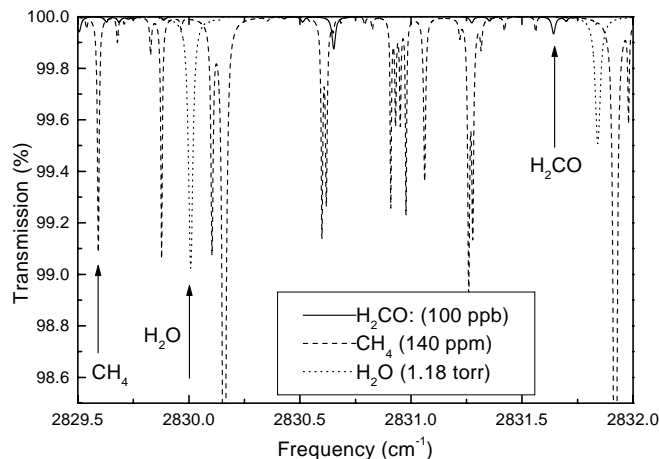


**Fig. 1.** HITRAN 96 simulation of the spectroscopic environment encountered in the vicinity of the  $2831.642\text{-cm}^{-1}$   $\text{H}_2\text{CO}$  absorption line selected for real-time monitoring of the air in the NASA Lunar–Mars life support chamber. The nearly isolated  $\text{CH}_4$  line is also shown. The spectroscopic parameters include: pathlength = 18 m, cell pressure = 60 Torr

its application. It is non-trivial to obtain an absolute measurement of absorption from modulation spectroscopy. We would have felt insecure unless we checked the calibration by periodically connecting an on-line reference gas to the multi-pass absorption cell for calibration of the system response. This would add to the overall sensor complexity.

## 1 Sensor configuration

A schematic of the DFG-based sensor is shown in Fig. 2. It is similar in design to that reported for CO detection previously [8]. The entire sensor including power supplies and electronics is contained in a  $30 \times 30 \times 65\text{ cm}$  enclosure weighing 25 kg. The infrared probe power is generated by mixing two cw narrow-bandwidth lasers (pump and signal) in periodically poled  $\text{LiNbO}_3$  (PPLN). The signal laser is a diode-pumped, non-planar monolithic ring Nd:YAG laser operating at a wavelength of 1064.5 nm and output power of 700 mW. The pump laser is a 100-mW GaAlAs Fabry–Pérot-

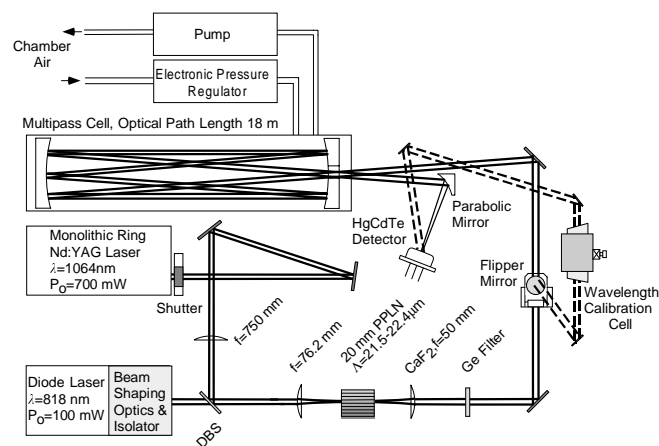


**Fig. 2.** Schematic of the cw mid-infrared DFG gas sensor. A compact diaphragm pump and electronic pressure regulator are used to provide on-line air sampling from the NASA chamber at reduced pressure

type diode laser at 818.0 nm. The diode laser is hermetically sealed in a TO-3 metal package together with a thermoelectric cooler and thermistor. The laser diode output beam is collimated with an  $f = 8$  mm multi-element lens, resulting in a 4-mm beam diameter in the long axis plane. The beam then passes through a 30 dB optical isolator, and a  $\lambda/2$  plate to rotate the polarization into the vertical phasematching plane. To achieve mode matching with the circular Nd:YAG laser beam, an anamorphic prism pair (4 $\times$ ) was used to reduce the vertical dimension of the laser diode beam. The two single longitudinal mode (SLM) pump beams were combined by a dielectric beam splitter mirror and focused into the PPLN crystal with a 75-mm focal length lens. The resultant beam diameters in the focal plane of the lens were measured to be 112  $\mu\text{m}$  ( $M^2 = 1.1$ ) and  $90 \times 109 \mu\text{m}$  ( $M_x^2 = 1.2$ ,  $M_y^2 = 5.3$ ) for the Nd:YAG and diode laser beams, respectively, (where  $M^2$  denotes the beam quality factor). To ensure overlap of the two pump beams at their waist in the PPLN crystal, a 75-cm focal length lens was placed in the 1064-nm beam path. The overlap of the two pump beams was optimized by means of a CCD-camera-based profiling system.

The predicted grating period for quasi-phasematching (QPM) of the incident wavelengths was 22.50  $\mu\text{m}$  at a temperature of 23  $^\circ\text{C}$ . The calculated temperature phasematching bandwidth of the DFG interaction was 16  $^\circ\text{C}\cdot\text{cm}$  (FWHM), using the Sellmeier equations in [15]. The PPLN crystal available for this experiment had grating periods ranging from 21.50  $\mu\text{m}$  to 22.40  $\mu\text{m}$  with 0.10- $\mu\text{m}$  channel increments (dimensions of 0.5 mm  $\times$  10 mm  $\times$  20 mm length). To improve the conversion with the non-optimum 22.40- $\mu\text{m}$  QPM period available, the grating was used at an incident angle of  $\approx 10^\circ$ , yielding an effective grating period of 22.46  $\mu\text{m}$ . Although crystal rotation increases the effective QPM period length to compensate for the shorter grating period used, a walk-off effect is introduced, which causes a reduction in beam overlap.

The generated mid-IR idler beam was collimated by a 5-cm focal length  $\text{CaF}_2$  lens, and the residual pump beams were removed by the use of an anti-reflection-coated Ge filter. The idler beam was then directed into a 0.3-l volume multi-pass absorption cell (New-Focus Inc, Model 5611). The cell was configured for 91 passes, corresponding to an optical path length of 18 m, and has a measured transmission of 20%. The DFG beam was then focused onto a thermoelectrically cooled HgCdTe (MCT) detector with a 1-mm<sup>2</sup> active area using a 5-cm focal length off-axis parabolic mirror.

To provide absolute frequency calibration, a  $\text{H}_2\text{CO}$  reference spectrum was acquired before every measurement. A computer-controlled mirror (New-Focus Inc., flipper) redirected the DFG beam through a 5-cm-long reference cell that contained 20 Torr of  $\text{CH}_4$  and a small amount of para-formaldehyde that was allowed to come to an equilibrium pressure in the gas mixture.

Unattended absolute concentration measurements require a reliable data acquisition system and control system that can perform mid-IR frequency scanning, sampling, frequency calibration, data analysis, and data storage. Frequency scans of the diode laser were obtained using a dedicated function generator circuit to modulate the diode current at 50 Hz with a 7.5-mA peak-to-peak triangular wave, corresponding to a scan range of 0.3  $\text{cm}^{-1}$ . The MCT detector was dc coupled to a preamplifier to allow absolute idler beam power measurements. The noise-equivalent power of the detector–

preamplifier combination was measured to be 3.9  $\text{pW Hz}^{-1}$ . The data was digitized and transferred to a laptop computer by use of a 16-bit A–D card (NI DAQCARD-AI-16XE-50). Data acquisition by the A–D card was synchronized to the laser diode current modulation with a TTL output available from the function generator.

Data analysis and experimental control was performed using LabVIEW software (National Instruments) on a laptop PC running Windows 95. For experimental control, two of the digital output lines from the A–D board were used to operate a beam shutter mounted in front of the Nd:YAG pump laser and the flipper mirror which redirected the DFG beam through the calibration cell. The shutter allowed the dark voltage of the MCT detector to be measured, which is necessary for absolute power measurements of the DFG beam.

The air in the NASA human-rated chamber was sampled in a continuous flow through the multi-pass absorption cell, by use of a compact 2-stage diaphragm pump (KNF Neuberger). The cell pressure could be regulated to lower pressures by use of an inline solid-state pressure regulator (MKS Instruments). The pressure was also additionally verified by use of an inline vacuum gauge adjacent to the multi-pass cell. The entire gas handling was contained within a small aluminum suitcase and connected to the chamber and sensor by use of 1/4-inch Teflon tubing. The chamber sample and return lines were approximately 6 m in length.

In order to remove high-frequency noise from the acquired scans a software-based low-pass Gaussian filter (with 1.3 kHz HWHM) was used. The positions of the acquired spectral features were obtained by applying a peak fitting routine to the  $\text{H}_2\text{CO}$  reference scan taken previously. Segments were removed from the base line that matched the estimated base width of each of the two  $\text{H}_2\text{CO}$  Lorentzian absorption peaks and the methane absorption peak. A fifth-order polynomial was then fitted to the remaining baseline to approximate 100% transmission at the  $\text{H}_2\text{CO}$  absorption peak. In addition, a Lorentzian lineshape was fitted to the principal  $\text{H}_2\text{CO}$  absorption line using a nonlinear least squares fit Levenberg–Marquardt method.

## 2 Experimental results and discussion

The detection sensitivity limit for this sensor was set by the occurrence of accidental etalons in the beam path, principally due to the laser diode window and collimation lens, the opto-isolator, the focusing lenses, the uncoated PPLN crystal surfaces, and the multi-pass cell. The etalon fringes from the multi-pass cell ( $< 10^{-4}$ ) could be reduced by manual vibration of the cell, however this was not required for general operation as the  $\approx 0.025\text{-cm}^{-1}$  period fringes had a minimal effect on the fitting algorithm accuracy. To reduce the effect from other etalons in the beam path on the accuracy of the calculated gas concentration, several data reduction techniques were employed. As mentioned above a fifth-order polynomial was fitted to the scan background, which partially normalized out etalon effects. In addition the knowledge of the position and width of the  $\text{H}_2\text{CO}$  absorption feature in each acquired scan permits a Lorentzian lineshape fit which is more accurate, thereby reducing aliasing by etalon fringes. The position of the  $\text{H}_2\text{CO}$  absorption line was determined by acquiring a reference  $\text{H}_2\text{CO}$  spectrum, prior to every experi-

mental scan. The width of the fitted Lorentzian curve was estimated using the theoretically predicted Lorentzian width from HITRAN 96. Furthermore it was seen that some of the etalon effects were transient, and predominantly due to thermal drifts of the sensor alignment induced by changes in the ambient temperature. Therefore averaging could also reduce etalon effects but at the expense of increased acquisition scans (typically 500 scans in 10 s. For longer-term monitoring the data was averaged over 2-h intervals).

The mid-IR power generated by the sensor at  $3.5\ \mu\text{m}$  was  $2.7\ \mu\text{W}$ , and after the multi-pass cell,  $0.42\ \mu\text{W}$  was incident on the detector. Typical operation of the sensor at NASA-JSC during the 3 weeks of the test involved one visit a day to optimize the alignment and frequency of the sensor and perform a periodic calibration check with a reference  $\text{H}_2\text{CO}$  sample of known concentration.

A spectral scan of the calibration cell ( $L = 5\ \text{cm}$ ) containing para-formaldehyde and 20 Torr methane over  $0.28\ \text{cm}^{-1}$  and centered at  $2831.6\ \text{cm}^{-1}$  is shown in Fig. 3 (1 s average). These scans were frequency calibrated to the frequency assignments [16] of two  $\text{H}_2\text{CO}$  absorption lines located at  $2831.6417$  and  $2831.6987\ \text{cm}^{-1}$ . The position of a  $\text{CH}_4$  line, which is obscured by one of the  $\nu_1$   $\text{H}_2\text{CO}$  lines, is also indicated in Fig. 3. From this pressure-broadened spectrum it is not possible to deduce the spectral bandwidth of the DFG radiation, because the total cell pressure is not known. However measurements of Doppler-broadened  $\text{CH}_4$  lines indicate a DFG bandwidth of  $\approx 100\ \text{MHz}$ . Shown in Fig. 4 is the spectrum of the same  $\text{H}_2\text{CO}$  absorption lines from an uncalibrated mixture of  $\text{H}_2\text{CO}$  in nitrogen, over an 18-m pathlength. The Lorentzian-lineshape fit to the data has a FWHM of  $0.027\ \text{cm}^{-1}$ , and yields an  $\text{H}_2\text{CO}$  concentration of 169 ppb (mole fraction). The etalon fringes in this scan represent  $\approx 0.025\%$  absorption which corresponds to a detection sensitivity of 36 ppb  $\text{H}_2\text{CO}$  for a  $S/N = 1$ .

For an accurate calibration of the  $\text{H}_2\text{CO}$  levels to be monitored, a  $67 \pm 1.5$  ppb calibrated mixture of  $\text{H}_2\text{CO}$  in nitrogen was used (H.P. Gas Products Inc). A time trace of the measured  $\text{H}_2\text{CO}$  concentration is shown in Fig. 5. In this cal-

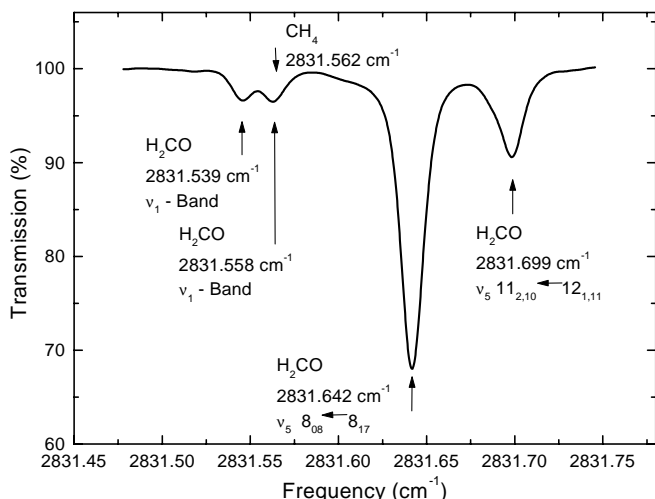


**Fig. 3.** Spectral calibration scan centered at  $2831.60\ \text{cm}^{-1}$  of a mixture of para-formaldehyde and 20 Torr methane over  $0.25\ \text{cm}^{-1}$  (1 s averaging). The  $\text{H}_2\text{CO}$  line at  $2831.6417\ \text{cm}^{-1}$  chosen for monitoring, the satellite  $\text{H}_2\text{CO}$  line at  $2831.699\ \text{cm}^{-1}$ , and an interfering  $\text{CH}_4$  line are shown

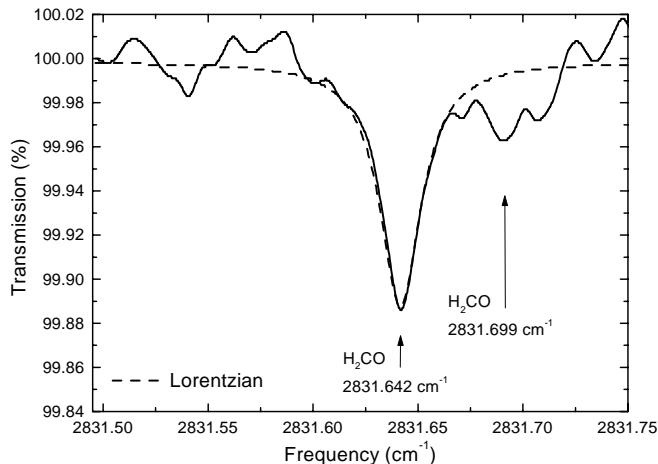


**Fig. 4.** Spectral scan of the  $\text{H}_2\text{CO}$  line at  $2831.642\ \text{cm}^{-1}$  of an uncalibrated mixture of  $\text{H}_2\text{CO}$  in nitrogen gas. An 18-m pathlength, cell pressure of 90 Torr and 5 s averaging time was used. The Lorentzian fit gives a  $\text{H}_2\text{CO}$  concentration of 169 ppb (mole fraction)

ibration the gas flowed continuously through the cell, which was regulated to 95 Torr. The  $\text{H}_2\text{CO}$  concentration was measured every 1 min. For each experimental point, the sensor first acquired a frequency calibration scan from the reference cell with 2 s of averaging, followed by 500 sweeps in 10 s of the gas in the multi-pass cell. Finally, the MCT dark voltage was acquired for 1 s. The average value of  $\text{H}_2\text{CO}$  absorption was measured for the last 33 min (after allowing the flowing  $\text{H}_2\text{CO}$  mixture to reach an equilibrium concentration with the gas tube walls). The standard deviation of the measurement was 13 ppb. This results in an absorption strength of  $4.67 \times 10^{-20}\ \text{cm}/\text{molecule}$  which compares well with the predicted absorption strength of  $5.04 \times 10^{-20}\ \text{cm}/\text{molecule}$  from the HITRAN 96 database.

A typical  $\text{H}_2\text{CO}$  and  $\text{CH}_4$  spectrum of the chamber air centered at  $2831.62\ \text{cm}^{-1}$  over a range of  $0.28\ \text{cm}^{-1}$  (960 data acquisition channels) is shown in Fig. 6. The linear power dependence resulting from the current modulation of the laser

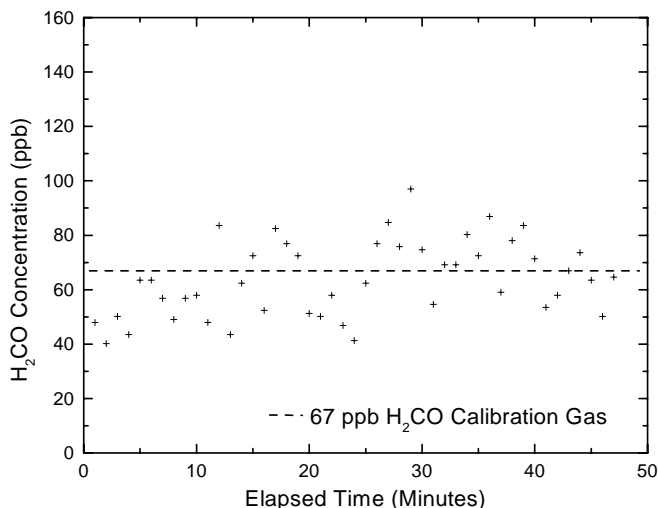


**Fig. 5.** DFG sensor calibration run based on monitoring the  $\text{H}_2\text{CO}$  concentration over a period of 50 min of a mixture of  $67 \pm 1.5$  ppb  $\text{H}_2\text{CO}$  in nitrogen gas. The measured  $\text{H}_2\text{CO}$  concentration was  $67 \pm 13$  ppb

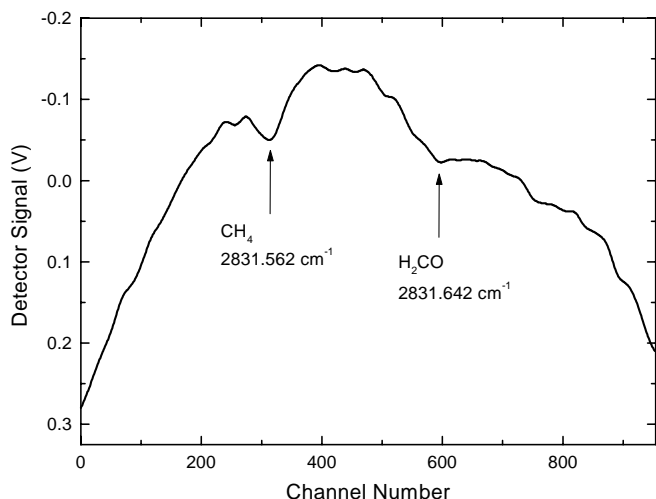


**Fig. 6.** Spectral scan over  $0.3 \text{ cm}^{-1}$  of the  $\text{H}_2\text{CO}$  line at  $2831.642 \text{ cm}^{-1}$  obtained using on-line air sampling from the NASA life support chamber: optical pathlength = 18 m, cell pressure = 95 Torr, 10 s averaging

diode has been removed in this figure, but it is otherwise unprocessed. The spectral positions of the  $\text{H}_2\text{CO}$  line of interest and interfering  $\text{CH}_4$  line are indicated. In Fig. 7 the baseline of the same  $\text{H}_2\text{CO}$  spectrum has been approximated using a fifth-order polynomial fit (excluding the absorption features), and the transmission has been normalized by means of the measured detector dark voltage. A Lorentzian lineshape has been fitted to the  $\text{H}_2\text{CO}$  peak ( $\text{CH}_4$  peak not fitted), resulting in a calculated concentration of 110 ppb (FWHM of  $0.036 \text{ cm}^{-1}$ ). In the fit a fixed Lorentzian lineshape width was used, and the Lorentzian center frequency was determined from the calibration scan. The residual from the Lorentzian fit is also shown, indicating the fringe noise to be  $\approx 0.02\%$ , consistent with the laboratory scan of  $\text{H}_2\text{CO}$  shown in Fig. 4.

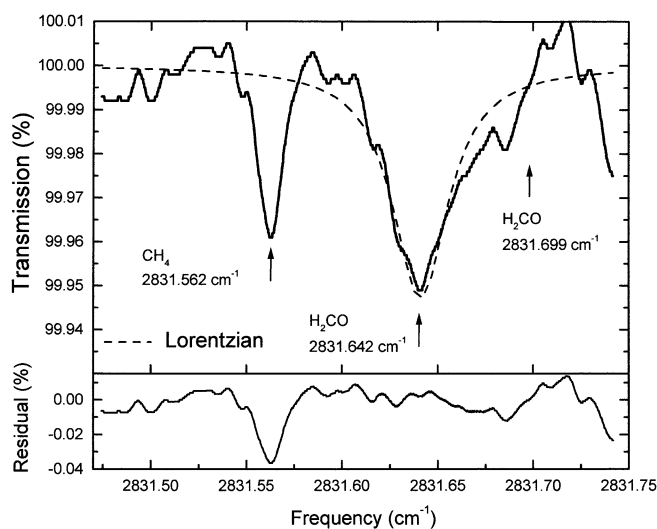


**Fig. 7.** The  $\text{H}_2\text{CO}$  spectrum derived from Fig. 6, with the absolute transmission calculated from the measured detector dark voltage, and the baseline normalized to 100% transmission using a fifth-order polynomial fit. The Lorentzian lineshape fit shown gives a  $\text{H}_2\text{CO}$  concentration of 93 ppb. A  $\text{CH}_4$  line near  $2831.562 \text{ cm}^{-1}$  is also shown. The residual from the Lorentzian lineshape fit is shown below  $\text{H}_2\text{CO}$  spectrum

The measured  $\text{H}_2\text{CO}$  concentration is shown in Fig. 8 for a time period of 21 h of unattended operation at NASA-JSC with a data collection scan taken every 7 min (scan started at 5 pm on December 17, 1997). During this time period the average  $\text{H}_2\text{CO}$  concentration measured was  $34 \text{ ppb} \pm 17 \text{ ppb}$  ( $\pm 1$  standard deviation,  $\sigma$ ). A power and frequency stability measurement of the sensor for this same 21-h period is shown in Fig. 9. The DFG power (measured after the multi-pass cell) decreased by 20%, which can be predominantly attributed to a thermally induced beam misalignment caused by a  $\approx 4 \text{ }^\circ\text{C}$  drop in temperature overnight in the building housing the test chamber. Verification of this beam misalignment was provided by the recovery of the power after this 21-h time period by optimizing the optical alignment. The DFG frequency drift was due to a temperature-induced drift of the laser diode frequency, and is within the specifications for the Peltier temperature controller for the diode laser. The change in the sensor alignment can produce a change in the etalon size and positions during a spectral scan. The  $0.03 \text{ cm}^{-1}$  frequency drift of the scan center frequency changes the portion of the baseline sampled and fitted. These two effects will influence the baseline fitting accuracy and introduce a slowly

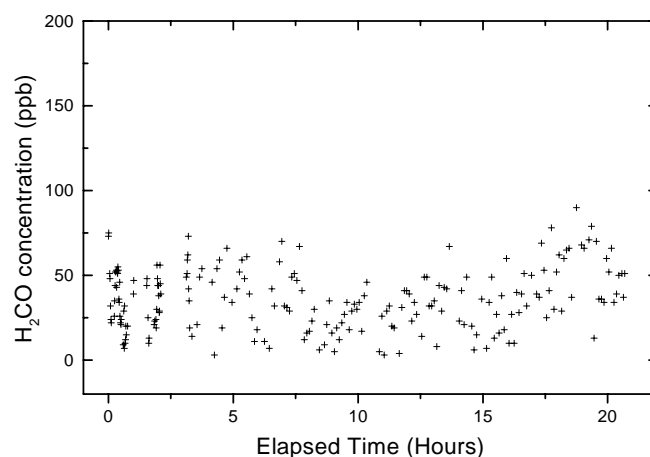


**Fig. 8.**  $\text{H}_2\text{CO}$  measurements conducted over a 21-h period, starting at 5 pm on December 17, 1997, of the air inside the NASA life support chamber (average measured is  $34 \pm 17 \text{ ppb}$ )

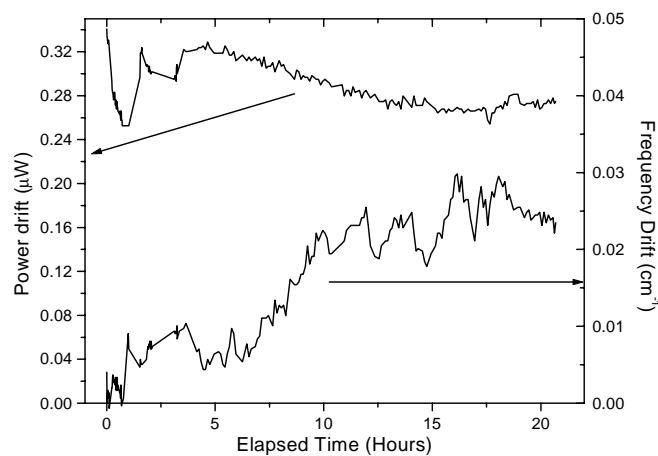


**Fig. 9.** Frequency stability and mid-IR power of the DFG based sensor for 21 h of operation starting at 5 pm on December 17, 1997

varying systematic offset in the  $\text{H}_2\text{CO}$  concentration in Fig. 8. The overall systematic error is estimated to be  $< 20$  ppb.

The measured  $\text{H}_2\text{CO}$  concentration for a 21-day period is shown in Fig. 10. Each point is an average of 2 h of collected data (approximately 60 measurements), and the error bars represent  $\pm 3\sigma_{\text{av}}$ , where  $\sigma_{\text{av}} = \sigma/(N)^{1/2}$ ,  $N = 60$ . Independent measurements of the  $\text{H}_2\text{CO}$  concentration were made by NASA-JSC personnel using chemically sensitized badges (also shown in Fig. 10), and show good agreement with our concentration measurements. As expected the  $\text{H}_2\text{CO}$  concentration measurements in the building verified that the sensor is recording the zero baseline within  $\pm 5$  ppb. The output of the trace contaminant control system (TCCS) in the chamber was also monitored, showing unexpectedly high  $\text{H}_2\text{CO}$  levels (Fig. 10). The interruption in monitoring from December 10 to 13, 1997, was the result of the failure of a pump laser and the time required for its replacement.

A measurement of  $\text{CH}_4$  concentration in the chamber required temperature tuning of the pump diode laser by  $1.3^\circ\text{C}$  to an isolated  $\text{CH}_4$  line at  $2829.592\text{ cm}^{-1}$ . Shown in Fig. 11 is a spectrum taken of the  $\text{CH}_4$  line at a cell pressure of 95 Torr and acquired using 5 s of averaging. For monitoring this line, the frequency was calibrated to a convenient nearby  $\text{H}_2\text{CO}$  line at  $2829.507\text{ cm}^{-1}$ , which could be observed in the calibration cell. The  $\text{CH}_4$  fitting algorithm simultaneously fitted a Lorentzian lineshape and a third-order polynomial, giving a  $\text{CH}_4$  concentration of 139 ppm. Methane concentration measurements made in a 27-h period starting on December 18, 1997, are shown in Fig. 12. Over the first 20 h we measured a  $\text{CH}_4$  level of  $140\text{ ppm} \pm 12\text{ ppm}$ . Verification of our  $\text{CH}_4$  measurement was provided by an on-line gas chromatography sensor reading a  $\text{CH}_4$  level of  $139\text{ ppm} \pm 1\text{ ppm}$  in the first hour of our measurements. The dramatic decline in  $\text{CH}_4$  concentration towards the end was due to the chamber door being opened at 21 h on December 19, 1997.

A spectrum of the  $\text{H}_2\text{O}$  line at  $2830.008\text{ cm}^{-1}$ , for a cell pressure of 100 Torr and 18-m pathlength is shown in Fig. 13. A Lorentzian fit (FWHM =  $0.024\text{ cm}^{-1}$ ) to the absorption peak gives a  $\text{H}_2\text{O}$  concentration of 13.0 parts per thousand, corresponding to 46.9% relative humidity at  $23^\circ\text{C}$ . Because

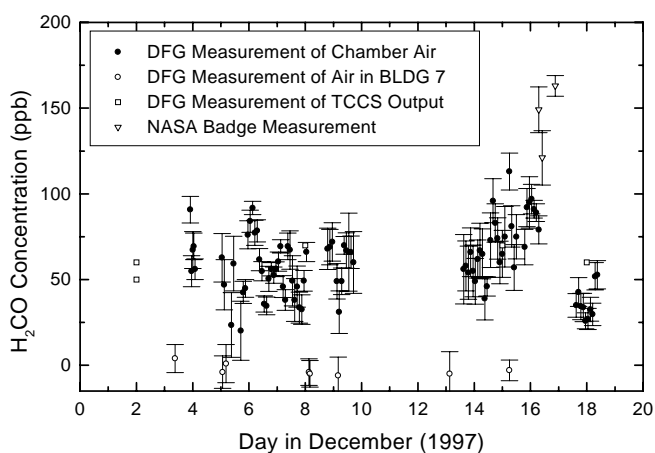


**Fig. 10.**  $\text{H}_2\text{CO}$  concentration in chamber air measured by the DFG sensor over 3 weeks from December 3 to 18, 1997. Each concentration point represents 2 h of data, and the error bars represent  $\pm 3\sigma_{\text{av}}$ . Independent measurements made of the  $\text{H}_2\text{CO}$  concentration by using a chemically based absorption badge measurement technique are also shown

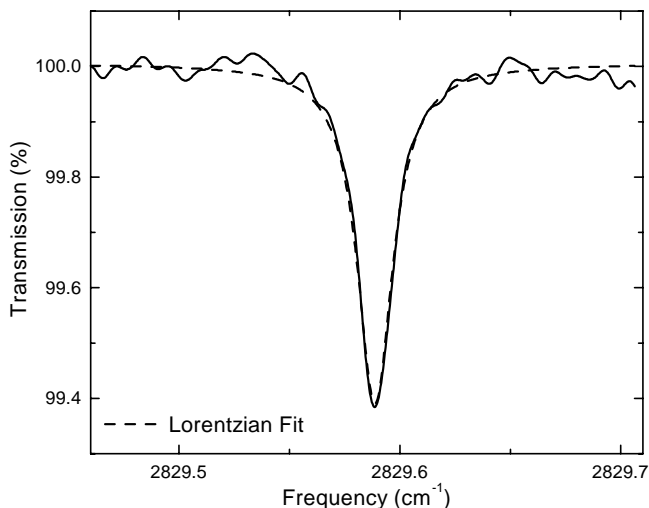


**Fig. 11.** Spectrum of a  $\text{CH}_4$  line at  $2829.592\text{ cm}^{-1}$  chosen for monitoring NASA chamber. Measured  $\text{CH}_4$  concentration is 139 ppm (cell pressure = 95 Torr,  $L = 18\text{ m}$ , 5 s averaging)

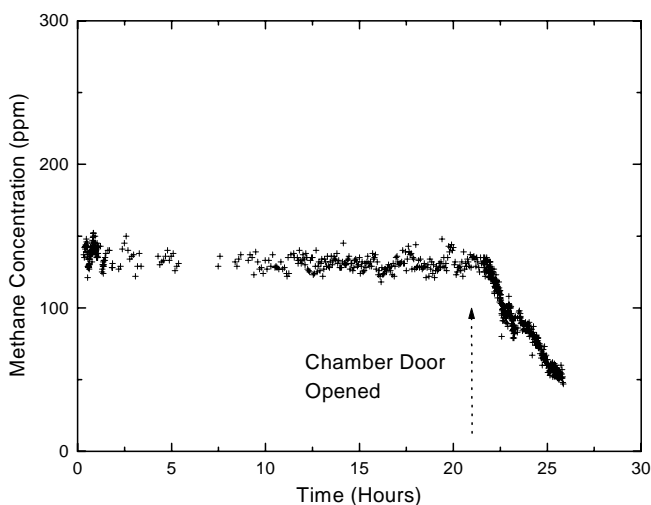


**Fig. 12.** Temporal trend of  $\text{CH}_4$  concentration in the NASA chamber air measured over 27 h. The chamber door was opened at 21 hours on December 19, 1997

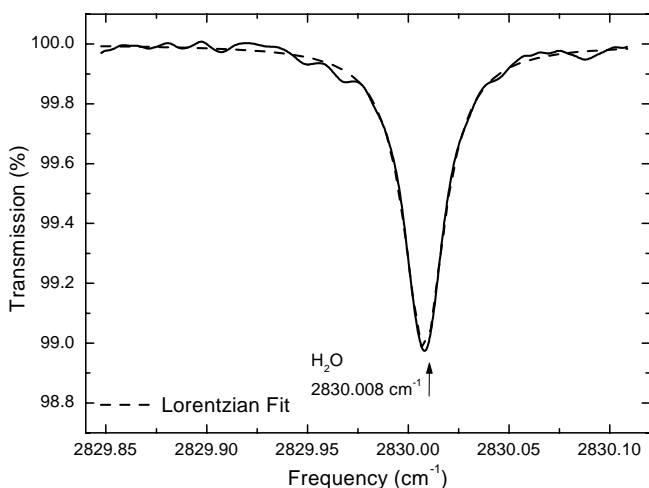


**Fig. 13.**  $\text{H}_2\text{O}$  spectrum of an isolated absorption line at  $2830.008\text{ cm}^{-1}$ . The measured  $\text{H}_2\text{O}$  concentration is 13.0‰, corresponding to 46.9% relative humidity at  $23^\circ\text{C}$  (cell pressure = 100 Torr,  $L = 18\text{ m}$ , 2 s averaging)

of the time constraints imposed by the length of the test, the H<sub>2</sub>O concentration was not measured inside the chamber.

The fitting techniques used were found to have a significant effect on the accuracy and scan-to-scan repeatability of the calculated concentrations, particularly for absorption measurements made near the sensitivity limit imposed by etalon effects in the beam path. The most effective fitting technique in terms of scan repeatability was found to be a simultaneous fit of the known lineshape characteristics and the baseline polynomial. In this work a single Lorentzian lineshape was fitted to the principal H<sub>2</sub>CO absorption line monitored at 2831.642 cm<sup>-1</sup>. However the presence of a satellite peak will introduce a systematic error in such a single-line Lorentzian fit. To improve the absolute concentration measurement, the principal H<sub>2</sub>CO peak and satellite peak should be fitted simultaneously with two Lorentzian lineshapes and the fifth-order polynomial. This modification will be implemented in future H<sub>2</sub>CO sensing applications. To improve the measurement accuracy, the systematic effects due to transient baseline features can be reduced by the use of frequent on-line H<sub>2</sub>CO calibrations.

The sensor has shown good stability over a period of several weeks and it can be made stable over much longer periods of time by implementing several new features. The most significant modification will be to minimize the occurrence and magnitude of etalons in the sensor, thereby increasing the detection sensitivity. The first step will be to add an anti-reflection coating to the PPLN crystal end faces. Besides reducing the etalon effect caused by the PPLN crystal, this will also increase the available DFG power, which in turn may permit a balanced detection scheme.

### 3 Conclusions

A tunable DFG sensor employed for on-line real time measurements of H<sub>2</sub>CO during a 1997 NASA Lunar Mars Life support test project has been described. The absolute calibration of the sensor was verified by using a 67 ppb H<sub>2</sub>CO in nitrogen mixture, with the sensor reading 67 ppb with a standard deviation of 13 ppb over 33 min. H<sub>2</sub>CO levels were measured to an accuracy of 30 ppb in a human-rated chamber over several weeks, and were in agreement with NASA-

conducted chemical badge measurements. Hence we have demonstrated that a DFG-based system using direct absorption spectroscopy can monitor near ppb concentrations (corresponding to absorptions of  $\approx 2 \times 10^{-4}$ ) of a trace gas over an extended period (several weeks), with the sensor operating in an industrial-type environment. This sensor incorporated several features for this purpose, including a computer-addressable reference cell and real-time data acquisition and processing. Furthermore, the detection capability of this sensor for multicomponent trace mixtures was demonstrated by temperature tuning of the pump diode laser to monitor CH<sub>4</sub> or H<sub>2</sub>O concentrations.

*Acknowledgements.* The authors would like to thank John Graf at NASA-JSC for support and helpful technical discussions. Financial support was provided by NASA, the Texas Advanced Technologies Program, the National Science Foundation, and the Welch Foundation. DR would like to acknowledge a stipend from the Deutscher Akademische Austauschdienst (DAAD).

### References

1. "Spacecraft Maximum Allowable Concentrations for Selected Airborne Contaminants", Vol. 1, Committee on Toxicology, NRC (National Academy Press, Washington DC 1994)
2. A. Fried, S. McKeen, S. Sewell, J. Harder, B. Henry, P. Goldan, W. Kuster, E. Williams, K. Baumann, R. Shetter, C. Cantrell: *J. Geophys. Res.* **102**, 6283 (1997)
3. M.W. Sigrist: *Air Monitoring by Spectroscopic Techniques* (Wiley, New York 1994)
4. D.M. Sonnenfroh, M.G. Allen: *Appl. Opt.* **36**, 7970 (1997)
5. S.I. Chou, D.S. Baer, R.K. Hanson: *Appl. Opt.* **36**, 3288 (1997)
6. M.S. Zahniser, D.D. Nelson, J.B. McManus, P. Kebejian: *Phil. Trans. R. Soc. Lond. A* **351**, 371 (1995)
7. M. Feher, P.A. Martin: *Spectrochim. Acta* **51A**, 1579 (1995)
8. T. Töpfer, K.P. Petrov, Y. Mine, D. Jundt, R.F. Curl, F.K. Tittel: *Appl. Opt.* **36**, 8042 (1997)
9. K.P. Petrov, R.F. Curl, F.K. Tittel: *Appl. Phys. B* **66**, 531 (1998)
10. A. Fried, S. Sewell, B. Henry, B.P. Wert, T. Gilpin, J.R. Drummond: *J. Geophys. Res.* **102**, 6253 (1997)
11. Y. Mine, N. Melander, D. Richter, D.G. Lancaster, K.P. Petrov, R.F. Curl, F.K. Tittel: *Appl. Phys. B* **65**, 771 (1997)
12. HITRAN 96, Ontar Corporation, North Andover, MA
13. D.S. Bomse, J.A. Silver, A.C. Stanton: *Appl. Opt.* **31**, 718 (1992)
14. X. Zhu, D.T. Cassidy: *J. Opt. Soc. Am. B* **14**, 1945 (1997)
15. D. Jundt: *Opt. Lett.* **22**, 1553 (1997)
16. L.R. Brown, R.H. Hunt, A.S. Pine: *J. Mol. Spectrosc.* **75**, 406 (1979)